

Elaboration of Certain lead-free ceramics of the perovskite type $Ba_{1-x} Y_{x/3} Bi_{x/3} (Ti_{0.65} Zr_{0.35}) O_3$

N.Boutal^(1,2), O.Boucenna⁽¹⁾, K.TAIBI²

(1) Department of Chemistry, Faculty of Exact sciences and Computer science, Seddik Ben Yahia University, Jijel, Algeria

(2) Crystallography-Thermodynamics Laboratory, Faculty of Chemistry, USTHB, Algeria,
e-mail: naimaboutal@yahoo.fr

Abstract— The ferroelectric materials currently used are lead-based ceramics. Such compounds are harmful to the environment due to the toxicity and volatility of lead oxide. Our work is done in the context of the protection of the environment. In this spirit new lead-free materials derived from $BaTiO_3$, by cationic substitutions in dodecahedral site were examined. The present study concerns compositions relatively close to $BaTiO_3$. Thus, we developed the compound $Ba_{1-x} Y_{x/3} Bi_{x/3} (Ti_{0.65} Zr_{0.35}) O_3$ ($x = 0.025$ and 0.05). The syntheses were carried out by reaction in the solid state. The purity of the phases obtained was checked by XRD. The study of the properties was carried out by dielectric measurements in temperature and frequency respectively in the ranges 77-400 K and 10^2 - $2 \cdot 10^5$ Hz.

Keywords— Ferroelectric, Relaxor, Lead-free perovskite, Céramic

I. Introduction

A large number of simple perovskite materials (ABO_3) exhibit a ferroelectric behavior. The substitution in the A and (or) B site of ABO_3 lattice lead to compounds of general formula $AA'BB'O_3$. In these complex perovskites, the statistical fluctuations of ions at the A and/or B-sites lead to local heterogeneity and large variations in the Curie temperature [1]. Depending on the substitution rate, these complex perovskites give rise to either normal ferroelectric or relaxor ferroelectric. The latter are distinguished by their particular dielectric performance characterized by a broad maximum with frequency dispersion and the temperature of the dielectric permittivity maximum shifts to higher values with increasing frequency. These characteristics make such materials excellent candidates for applications as capacitors and actuators [2]. However, the majority of relaxor materials are lead-based ceramics and this causes serious environmental problems due to the high toxicity and volatility of lead oxide. Therefore, to develop environment friendly materials, lead free compositions were examined. Among the congeners, $Ba_{1-x} Y_{x/3} Bi_{x/3} (Ti_{0.65} Zr_{0.35}) O_3$ (BYBiZT) ($x=0.025$ $x=0.050$) ceramics are interesting owing to their attractive ferroelectric performances. In fact, the substitution of Ti by Zr in the B site exhibits for some compositions, relaxor properties near room temperature [3]. It has also been shown, that heterovalent substitutions in the A site coupled to homovalent substitution in the B site could induce the coexistence between order (ferroelectric) and disorder (relaxor) leading to an increase of the degree of relaxor behavior [4]. On the other hand, the relaxors present large dielectric constants and wide space charge region.

compounds $Ba_{1-x} Y_{x/3} Bi_{x/3} (Ti_{0.65} Zr_{0.35}) O_3$. The compositions were obtained by coupling heterovalent substitution in the A-site (Ba^{2+}/Bi^{2+} et Y^{3+}) and homovalent substitution in the B-site (Ti^{4+}/Zr^{4+}).

II. Experimental

II.1. Results and discussion

II.1.1. The compound $A_{1-x}A'xTiO_3$ ($A= Ba$; $A'= Y$)

$Ba_{1-x}Y_{2x/3}TiO_3$ has a tetragonal structure for $x < 0.059$. The thermal and frequency evolution of ϵ'' and ϵ''/ω ($0.028 \geq x > 0.059$ and cubic for $x < 0.258$) shows the presence of a peak with frequency dispersion for $x > 0.028$ and whose maximum decreases as the amount of yttrium increases. The temperature corresponding to this maximum decreases linearly with a gap of 29 K for $y < 0.122$ and then remains constant for $y > 0.122$. A typical relaxor behavior is observed and becomes more significant as the yttrium concentration increases [5, 6].

For this solid solution, we used a formulation assuming substitution at site A in the range $0 < x < 0.10$. In this case, the XRD study showed that the phases obtained were pure for $x < 0.10$.

The dielectric study revealed classic ferroelectric behavior whatever the compositions for $x < 0.10$.

By way of example, Figures (1) and (2) show, respectively, the thermal evolution of ϵ'_r and $1/\epsilon'_r$ for ceramic of composition $Ba_{0.95}Y_{0.033}TiO_3$. Furthermore, as the amount of yttrium increases, the transition temperatures T_1 , T_2 and T_3 remain virtually constant. Despite the size difference between the substituted cations, the replacement of Ba^{2+} by Y^{3+} has virtually no influence on the electrical properties of $BaTiO_3$. Indeed, instead of decreasing, T_c remains virtually constant when Y^{3+} is added. We have attempted to explain this anomaly by fact that Y^{3+} (very small in size compared with Ba^{2+}) was also likely to substitute in the octahedral site [7]. If this were the case, there would be an increase in size and a decrease in charge corresponding to the transition from Ti^{4+} to Y^{3+} ($r_{Y^{3+}} = 0.90 \text{ \AA}$ and $r_{Ti^{4+}} = 0.605 \text{ \AA}$ in coordinate 6 [8] and would lead to a decrease in T_c . This anomaly was then attributed to the creation of gaps within the cristal lattice due to the difference in charge between Ba^{2+} and Y^{3+} .

In fact, when moving from Ba^{2+} to Y^{3+} , the number of vacancies increases, influencing cationic order. The presence of these vacancies lead to disordered structures (Δz increases) and consequently to higher value of T_c [9]. These two contradictory effects lead to virtually constant T_c values.

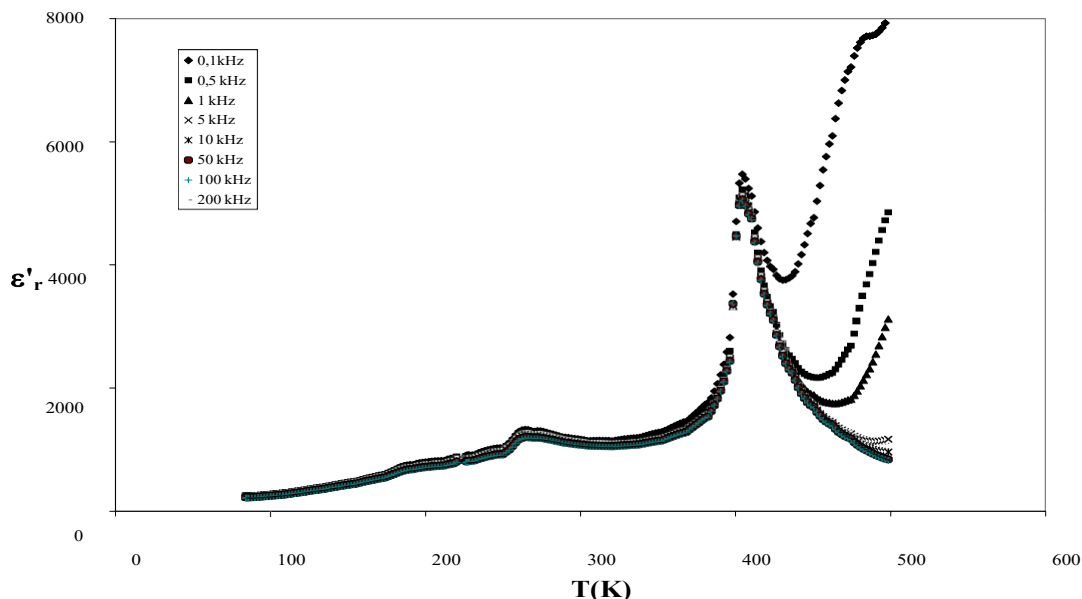


Fig.1 Thermal variation of ϵ'_r for a ceramic with composition $Ba_{0.975} Y_{0.0166}TiO_3$

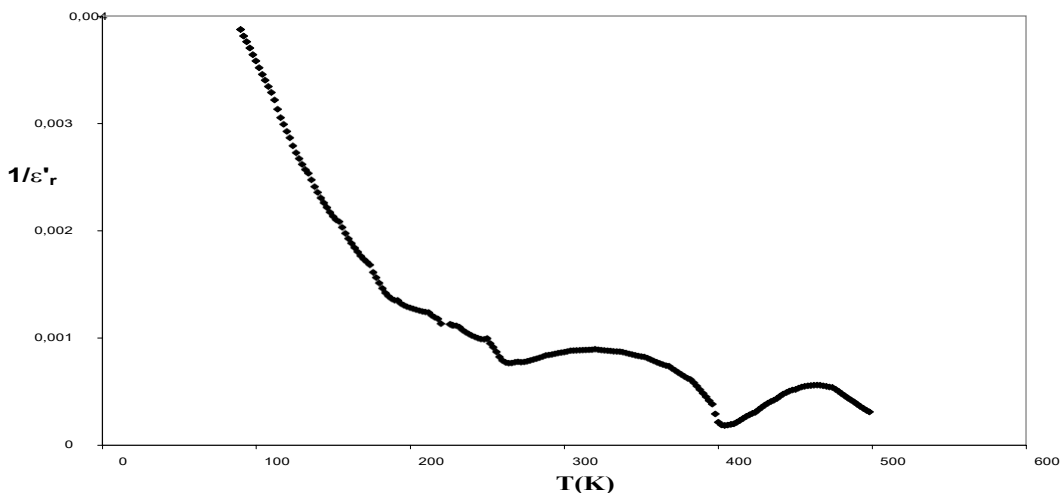


Fig.2: Thermal variation of $1/\epsilon'_r$ for a ceramic with composition $Ba_{0.975} Y_{0.017}TiO_3$

2.2- Compounds $A(B_{1-y}B'_y)O_3$ ($A=Ba$; $B=Ti$ and $B'=Zr$)

This involves homovalent substitution of Ti^{4+} by ions of the same charge such as Zr^{4+} .

Various single-phase compositions of the formula $Ba(Ti_{1-y}Zr_y)O_3$ for $0,26 < y < 0,40$ a diffuse phase transition with frequency dispersion is obtained. In addition, there is a deviation from the curie-weiss law. In this range, permittivities are of the order of 5000 at 1 kHz. Furthermore, the characteristic parameters (Tab.1) clearly show the presence of diffuse phase transitions in the range $0,30 \leq y \leq 0,40$.

Table.1: Characteristics of ceramic relaxers with formula $Ba(Ti_{1-y}Zr_y)O_3$ [10].

y	$\Delta\epsilon'_r / \epsilon'_r$	T_m (K)	ΔT_m (K)
0,30	0,19	240	6
0,35	0,43	200	10
0,40	0,56	190	16

XRD and SEM investigations revealed the following observations :

- The solid solution obtained are perfectly pure. The corresponding diffractograms show a single perovskite-like phase, comparable to the cubic variety of $BaTiO_3$ (**Fig.3**).

The diagrams for these solid solutions were isotypically indexed on the cubic phase of $BaTiO_3$ using the Dhkl program. After an approximate calculation, the mesh parameters were refined by the last-squares method using AFPAR software [11].

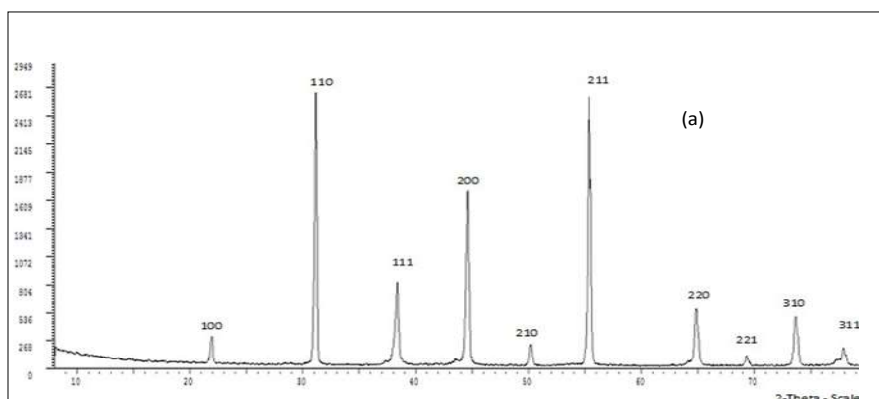
- **Fig.4** shows the evolution of mesh parameters (a) and mesh volume (b) as a function of composition. Replacing the Ti^{4+} ion with the Zr^{4+} ion leads to an increase in mesh parameters and volume. This extension of the mesh is linked to the large size of Zr^{4+} compared with Ti^{4+} ($r_{Zr^{4+}}=0,720 \text{ \AA}$ and $r_{Ti^{4+}}=0,605 \text{ \AA}$ in coordinate 6 [8]).

- Scanning electron microscopy shows that our products were synthesized under good conditions. The microstructure is relatively dense and inhomogeneous. Grain size varies between 0.2 and 0.3 μm (Fig.4). Moreover, the largest sizes are obtained for composition with high y values. This is in line with the difficulty of substituting Ba^{2+} by Zr^{4+} for y values greater than 0.4.

Dielectric measurements are given the results shown in **fig.5**. These illustrate the temperature and frequency variations in real (ϵ'_r) and imaginary (ϵ''_r) relative permittivities for the solid solution with composition $y=0.35$.

A single diffuse peak appears, whose maximum permittivity temperature (T_m) increases with frequency. This frequency dispersion is only apparent in the ferroelectric phase: as frequency increases, ϵ'_r decreases ϵ''_r , and increases, $\epsilon''_{r(max)}$ and $\epsilon''_{r(max)}$ the temperature of and increases. We also observe greater dispersion with higher substitution rates: ΔT_m varies from 6 K (for $y=0,30$) à 16 K (for $y=0,40$) [9]. In this case of our compositions ΔT_m varies from 5 K (for $y=0.30$) to 30 K (for $y=0.40$).

On the other hand, the thermal variation of $1/\epsilon'_r$ (**fig.8**) shows a significant deviation from the Curie-Weiss law. Strong curvature of $1/\epsilon'_r$ around T_m is characteristic of a diffuse phase transition. All these observations indicate that the solid solutions $Ba(Ti_{1-y}Zr_y)O_3$ exhibit ferroelectric-relaxing behavior.



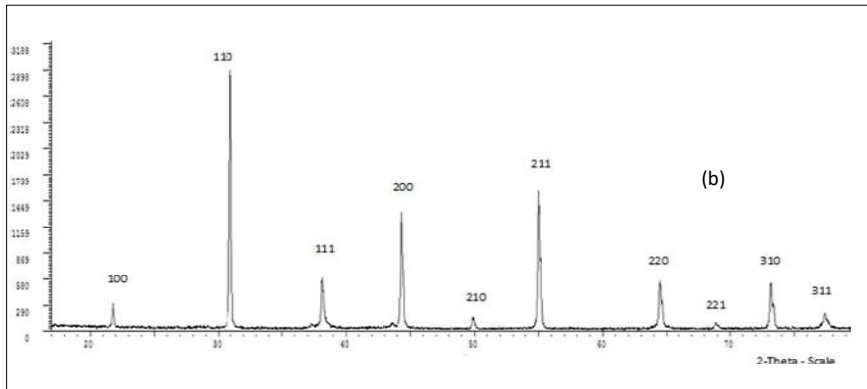


fig.3. powder x-ray diffraction of $Ba(Ti_{1-y}Zr_y)O_3$ $y = 0,30$ (a) et $y = 0,40$ (b)

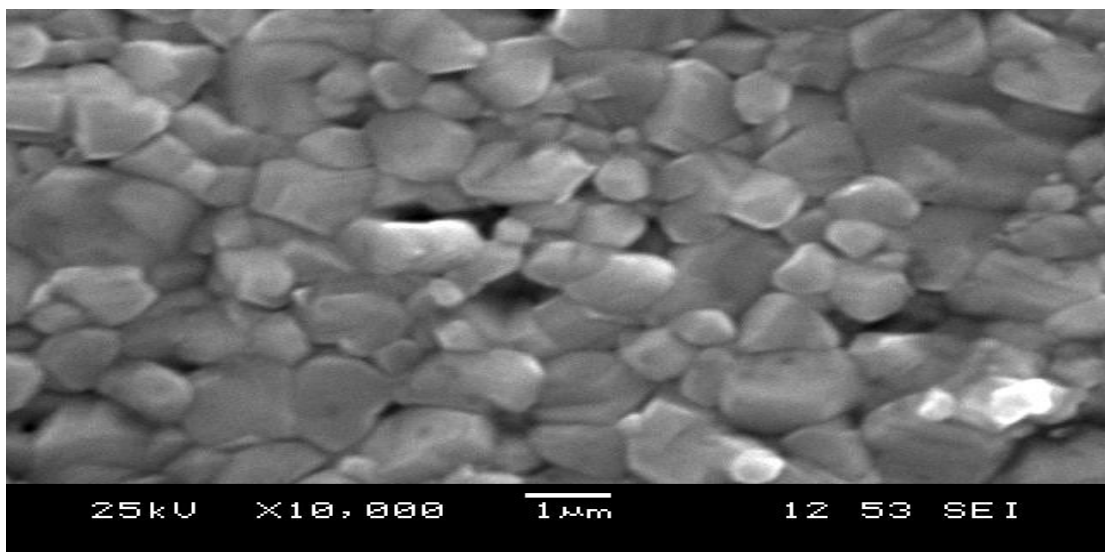


Fig.4 .Phase micrograph OF $Ba(Ti_{1-y}Zr_y)O_3$ $y=0, 30$

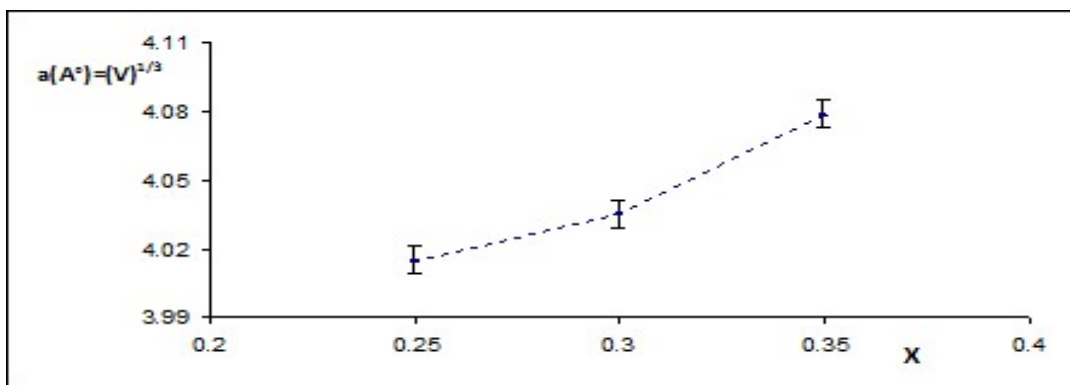


Fig. 5. Evolution of the parameter and volume of the mesh depending on the composition in the phase $Ba(Ti_{1-y}Zr_y)O_3$

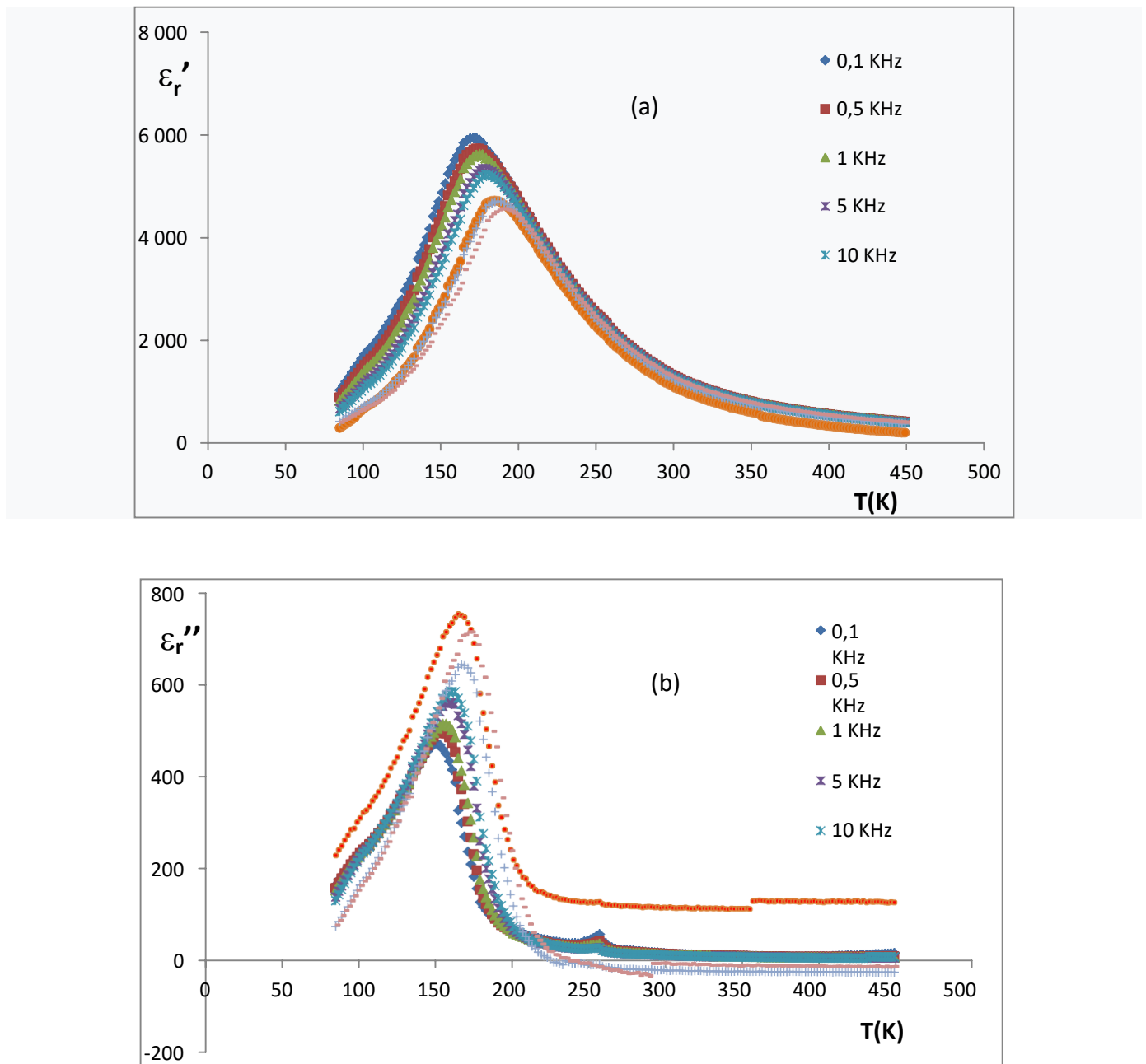


Fig.6. Temperature and frequency dependences of real and imaginary parts of the permittivity ϵ_r for a ceramic with the composition $\text{Ba}(\text{Ti}_{0,65}\text{Zr}_{0,35})\text{O}_3$

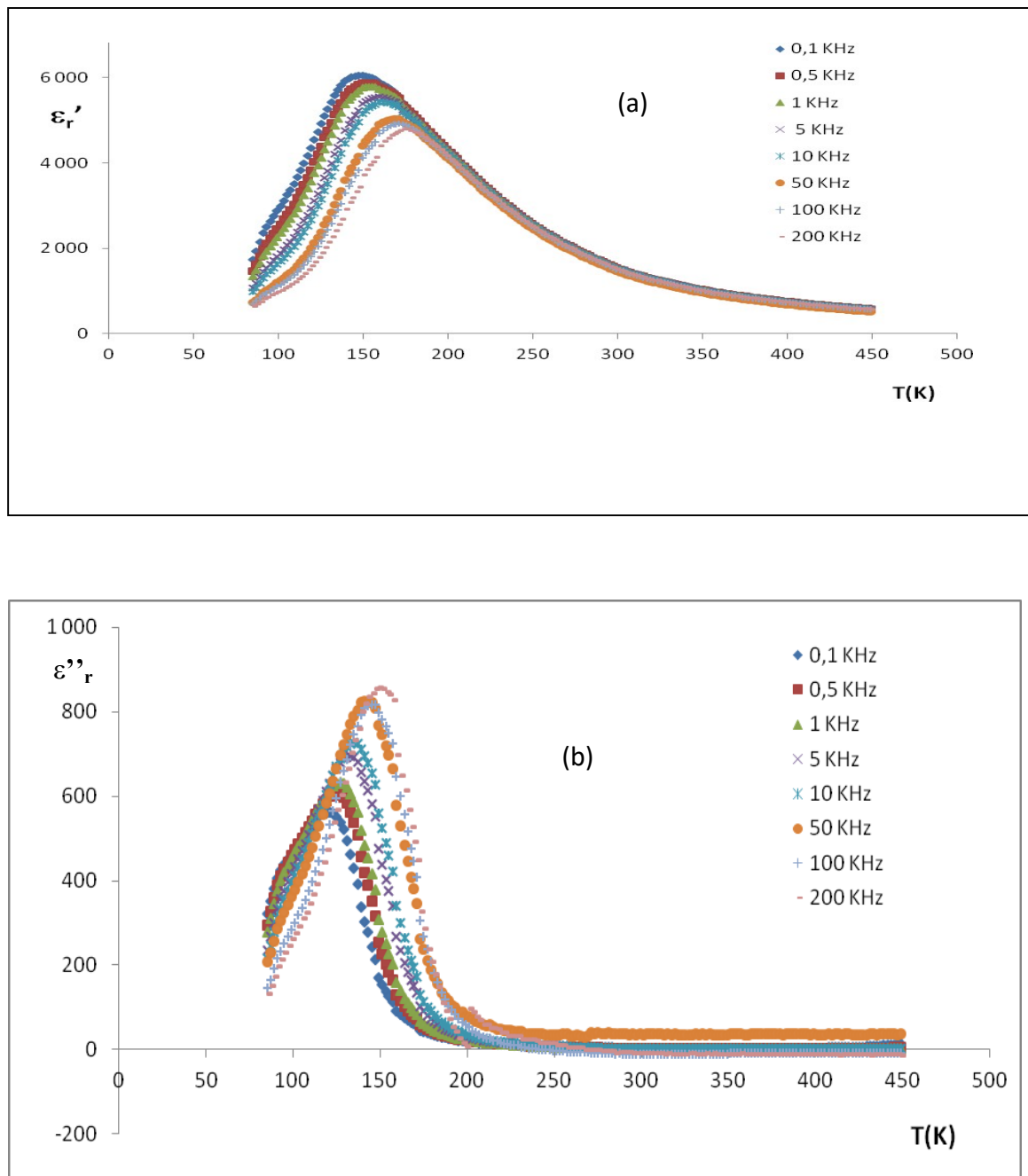


Fig.7. Temperature and frequency dependences of real and imaginary parts of the permittivity ϵ_r' for a ceramic with the composition $\text{Ba}(\text{Ti}_{0,65}\text{Zr}_{0,35})\text{O}_3$

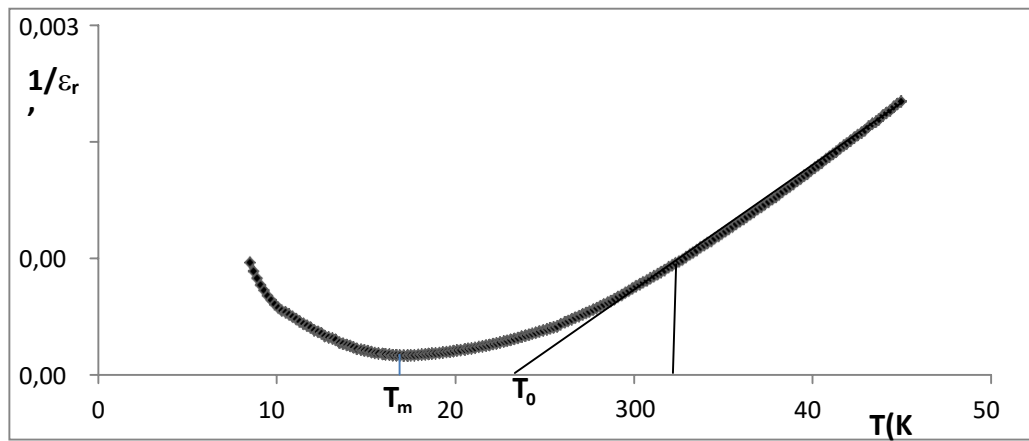
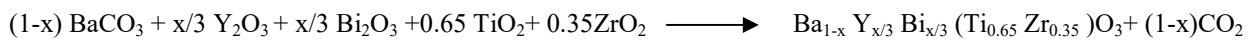


Fig.8.thermal evolution of the inverse of the real relative permittivity for the phases $\text{Ba}(\text{Ti}_{0.65}\text{Zr}_{0.35})\text{O}_3$ ($f=1\text{KHz}$)

II.3.The compounds $(\text{A}_{1-x}\text{A}'_{x/3}\text{B}_{1-y}\text{B}'_y)\text{O}_3$ ($\text{A} = \text{Ba}$; $\text{A}' = \text{Y, Bi}$; $\text{B} = \text{Ti}$ et $\text{B}' = \text{Zr}$)

II.3.1.Solid-state synthesis

The starting compounds were powders of BaCO_3 , TiO_2 , ZrO_2 , Y_2O_3 and Bi_2O_3 (all of Sigma Aldrich)(table.2). Materials with compositions $\text{Ba}_{1-x}\text{Y}_{x/3}\text{Bi}_{x/3}(\text{Ti}_{0.65}\text{Zr}_{0.35})\text{O}_3$ were synthesized in the range $0.025 \leq x \leq 0.050$ by the conventional mixed oxide method from BaCO_3 and dry oxides (TiO_2 , ZrO_2 , Y_2O_3 and Bi_2O_3), all of analytical quality according the following chemical scheme:



The compositions $\text{Ba}_{1-x}\text{Y}_{x/3}\text{Bi}_{x/3}(\text{Ti}_{0.65}\text{Zr}_{0.35})\text{O}_3$ are non-stoichiometric due to the difference of charge between Ba^{2+} and Y^{3+} , located in the dodecahedral site. Weighed ingredients were wet mixed for 2 h and calcined at 850°C for 12 h. After new intimate and ground mixings, the calcined powders were pressed under 100 MPa into disk of 8 mm diameter and 1 mm thickness. Disk shaped ceramics were then sintered at 1150°C for 4 h. Loss weight systematically determined before and after heat treatment was less than 1%. Diameter shrinkages DU/U were determined as $(\text{U}_{\text{initial}} - \text{U}_{\text{final}})/\text{U}_{\text{initial}}$. Their values were in the range 0.10–0.15 while the compactness (experimental density/ theoretical density) was about 0.96.

2.2. Characterization

To determine the phase composition, symmetry and unit cell parameters, X-ray powder diffraction (XRD) was used. The data were collected at room temperature with a PaNalytical X'Pert PRO MPD diffractometer using $\text{Cu K}\alpha 1$ radiation ($\lambda = 1.5406^\circ$) in the 2θ range ($10\text{--}80^\circ$) and steps of 0.02° with 10s counting time for each step.

Dielectric measurements were performed on the ceramic disks after depositing gold electrodes on the circular faces by dc sputtering. The real and imaginary parts of the permittivity ϵ'_r and ϵ''_r were measured under helium atmosphere as a function of both temperature (75–450 K) and frequency (102–2- 105 Hz) using a Wayne–Kerr 6425 component analyzer.

Product	Brand and purity	Product	Brand and purity
BaCO ₃	(Merck, 99,9%)	TiO ₂	(Aldrich, 99,9%)
ZrO ₂	(Aldrich, 99,9%)	Y ₂ O ₃	(Aldrich, 99,9%)
Bi ₂ O ₃	(Aldrich, 99,9%)		

TABLE I: CHARACTERISTICS OF STARTING PRODUCT

II.3.3. Results and discussion

XRD study

The powders were weighted, mixed for 2 h and calcined during 12 h at 850°C (BBiYT). After new intimate and ground mixings, the calcined powders were pressed under 100 MPa into disk of 8 mm diameter and 1 mm thickness. Disk shaped ceramics were then sintered under oxygen atmosphere for 4h at 1150°C (BBiYT).

The X-Ray Diffraction (XRD) data were collected with a Panalytical X'Pert PRO MPD diffractometer using Cu K α radiation ($\lambda = 1.5406 \text{ \AA}$) in the range (5–80°) and steps of 0.02° with 10 s counting time for each step.

Room temperature XRD analyses allow us to determine the limits of the solid solutions in which the structural type is kept as perovskite. The patterns of Ba_{1-x}Y_{x/3}Bi_{x/3}(Ti_{0.75}Zr_{0.25})O₃ compositions are characteristics of a cubic symmetry (Fig.9). The XRD profiles reveal that:

For $x = 0.025$, no parasite phase exists; only peaks corresponding to the perovskite phase are present. From $x = 0.050$, despite the optimal conditions for elaboration, some very weak peaks corresponding to impurities take place beside the Bragg reflexions. The presence of these impurities is certainly related to the weak solubility of rare earth in the A site [12].

Dielectric measurements were performed on the ceramic disks after depositing gold electrodes on the circular faces by dc sputtering. The permittivity ϵ_r' was measured under helium atmosphere as a function of both temperature (75–450 K) and frequency (10²-2.10⁵ Hz) using a Wayne-Kerr 6425 analyzer.

For the solid solutions Ba_{1-x}A_{2x/3}A'_{x/3}(Ti_{0.7}Zr_{0.3})O₃ (A = Bi, A' = Y), progressive substitutions in the dodecahedral sites of Ba²⁺ cations by Bi³⁺ or Y³⁺ cause a decrease in the volume V and lattice parameter as x increases. These variations are consistent with the size of the substituted ions (r Ba²⁺ = 1.42 Å; r Bi³⁺ = 1.17 Å in coordination 8). However, an inverse evolution is observed in the case of compounds containing yttrium. Although Y³⁺ has a smaller radius than that of Ba²⁺ (r Y³⁺ = 1.019 Å in coordination 8), the lattice parameter increases as the amount of Y³⁺ (and consequently x) grows. This variation contradicts the ion size evolution when Y³⁺ replaces Ba²⁺, assuming these ions occupy the same crystallographic site. It is likely that, due to their smaller size, Y³⁺ ions not only substitute for Ba²⁺ (in site A) but also for Ti⁴⁺ or Zr⁴⁺ (in site B). In this case, increases in lattice parameter and volume with x can be explained.

During the course of this study, we have examined coupled substitutions at sites A and B, specifically the compositions of Ba_{1-x}Bi_{x/3}Y_{x/3}(Ti_{1-y}Zr_y) for $x = .025$; .050 and $y = .35$. This involves the heterovalent substitution of bismuth for barium and yttrium alongside the homovalent substitution of zirconium for titanium. These substitutions are important in understanding the properties and behavior of materials in various applications, and our findings contribute to a better understanding of these complex systems.

The phases obtained are pure for $x = .025$. However, despite the optimal choice of processing conditions, at the value $x = .050$, some impurity lines appear next to the Bragg peaks. (Fig.9) shows the diffraction patterns obtained for the compositions Ba_{1-x}Bi_{x/3}Y_{x/3}(Ti_{1-y}Zr_y) for $x = .025$ (a); .050 (b) and $y = .35$.

The presence of these impurities can be attributed to the fact that these rare earth elements have a low solubility in site A of perovskites and they are generally likely to be incorporated simultaneously in sites A and B.

Understanding and addressing these impurities are crucial for controlling material properties and ensuring their reliable performance in practical applications.

We have conducted the dielectric measurements and discovered the presence of the relaxor phenomenon across all compositions explored. Furthermore, we observed that the diffuseness of the transition (relaxor character) predominantly amplifies with an increase in substitution rate at site B (as y increases). Fig.10 and 11 depict the temperature and frequency variations of real (ϵ_r') and imaginary (ϵ_r'') relative permittivities for ceramics with formulas Ba_{1-x}Bi_{x/3}Y_{x/3}(Ti_{0.65}Zr_{0.35}) for $x = 0,025$ (a); 0,050 (b), and $y = 0,35$.

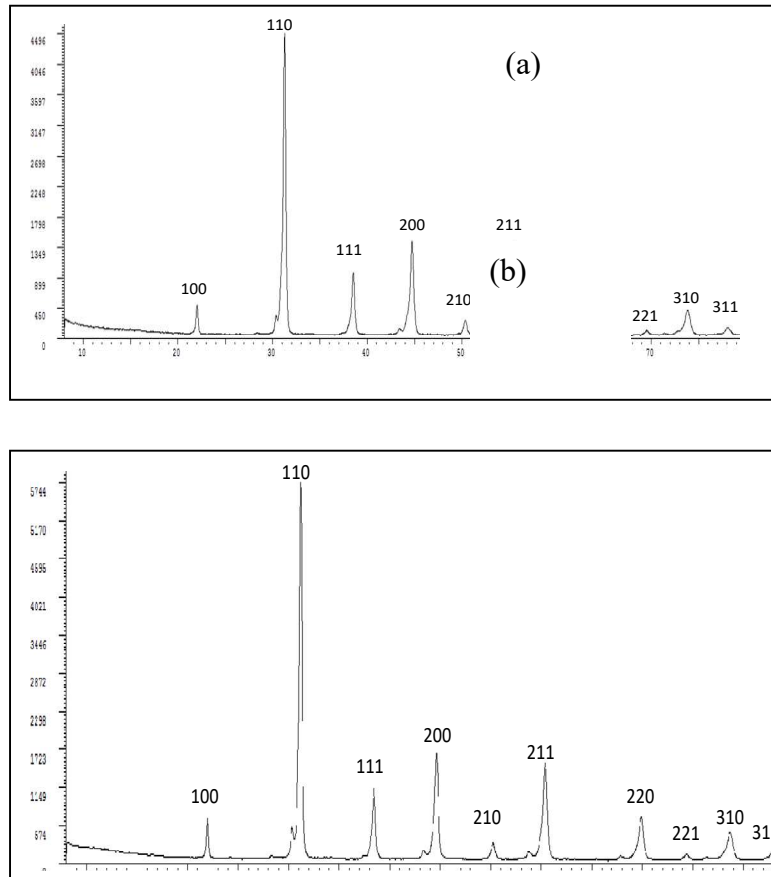
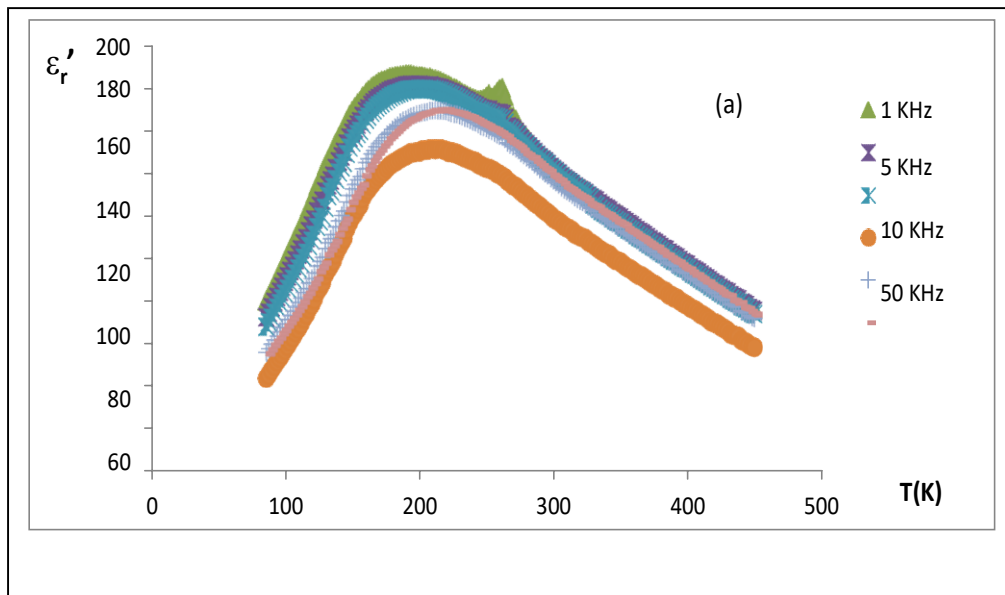


Fig.9. powder x-ray dffraction of $Ba_{1-x}Bi_xY_{x/3}(Ti_{0.65}Zr_{0.35})O_3$ ($X=0,025(a)$ et $X=0.050(b)$)



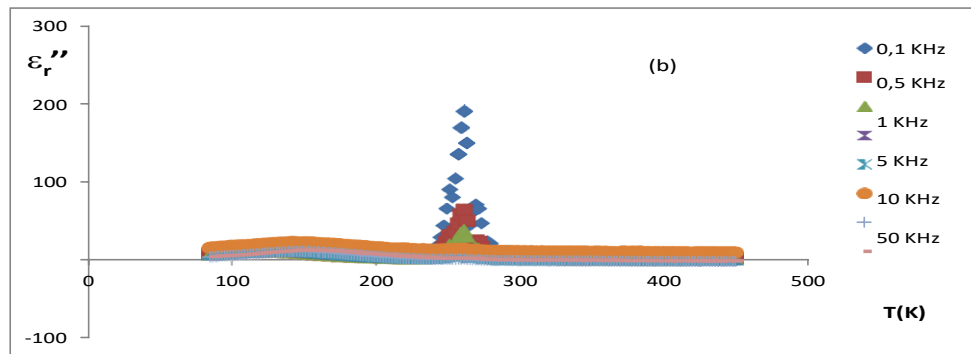


Fig.10. Temperature and frequency dependences of real and imaginary parts of the permittivity ϵ_r for a ceramic with the composition $Ba_{1-x}Bi_{x/3}Y_{x/3}(Ti_{0.65}Zr_{0.35})O_3$ ($X=0,025$)

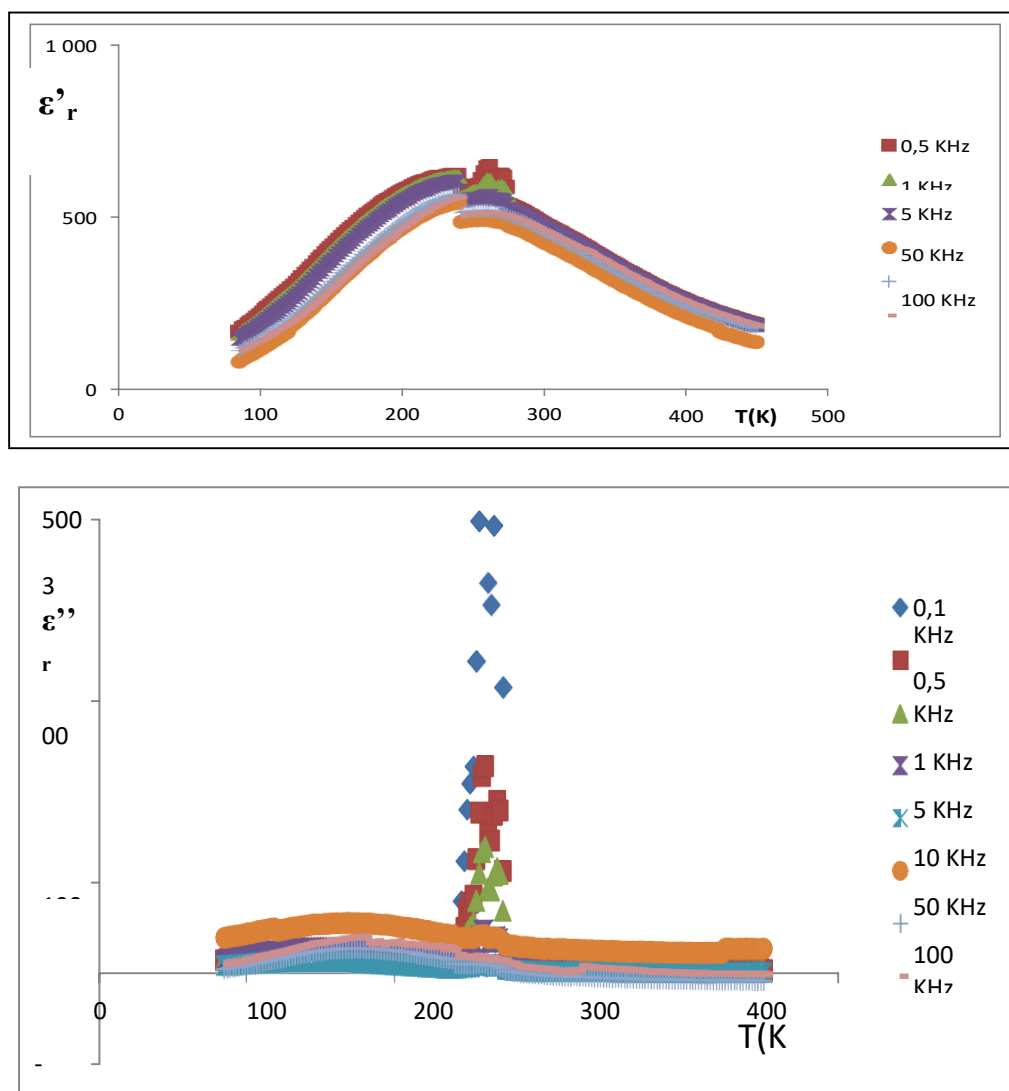


Fig11. Temperature and frequency dependences of real and imaginary parts of the permittivity ϵ_r' for a ceramic with the composition $Ba_{1-x}Bi_{x/3}Y_{x/3}(Ti_{0.65}Zr_{0.35})O_3$ ($X=0,050$)

On the other hand, the thermal variation of $1/\epsilon_r'$ (**fig.12**) shows a significant deviation from the Curir-Wiess law.

Strong curvature of $1/\epsilon_r'$ around T_m is characteristic of a diffuse phase transition. All these observations indicate that the solid solutions $Ba_{1-x}Bi_{x/3}Y_{x/3}(Ti_{0,65}Zr_{0,35})O_3$ exhibit ferroelectric-relaxing behavior.

I appreciate the detailed analysis and observations regarding the thermal variation and phase transition behavior of the material in fig 12. Your insights into the deviation from the Curie-Weiss law and the characteristic features of a diffuse phase transition are quite informative.

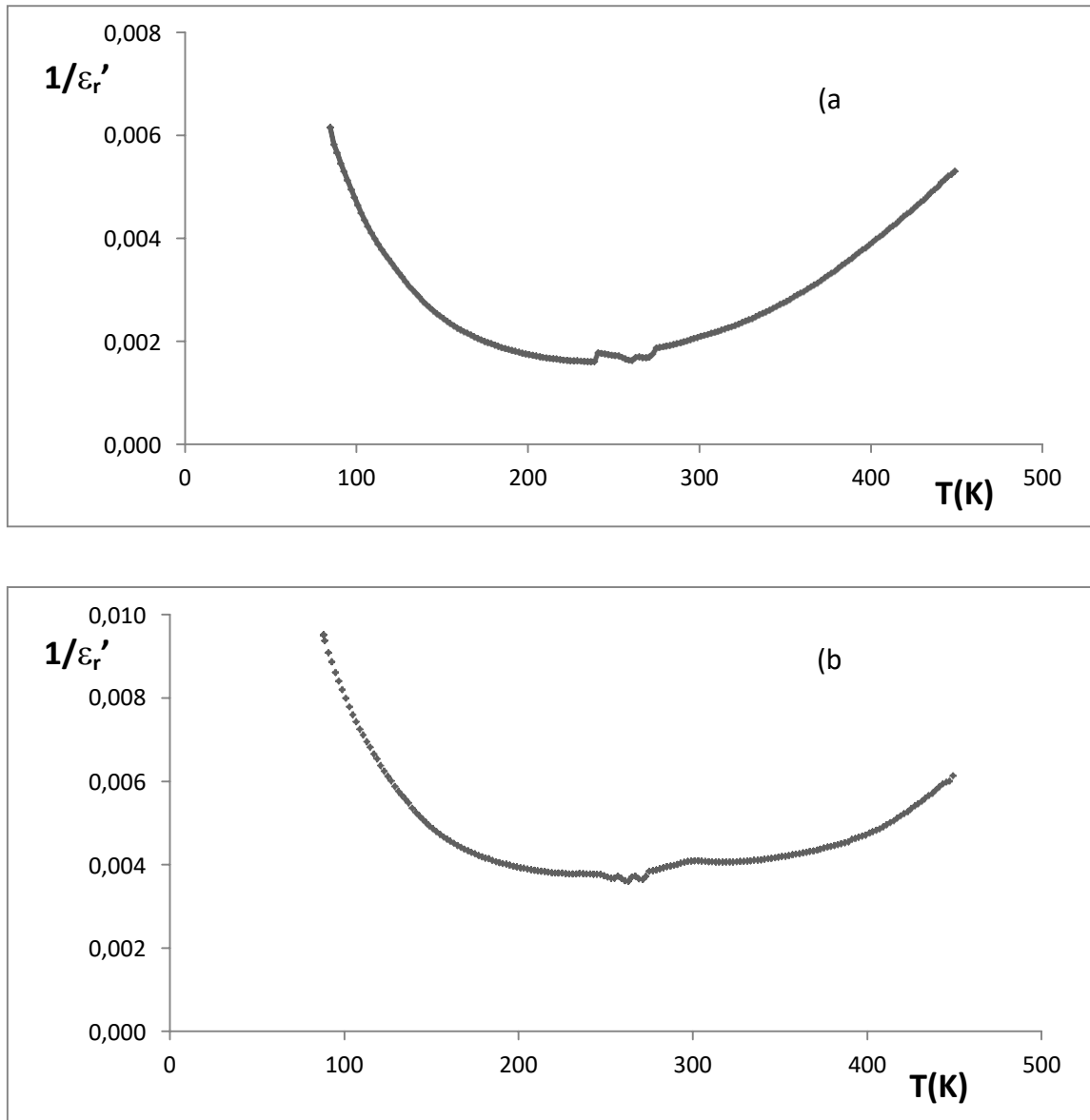


Fig.12.thermal evolution of the inverse of the real relative permittivity for the phases $Ba_{1-x}Bi_{x/3}Y_{x/3}(Ti_{0,65}Zr_{0,35})O_3$ (a) $x=0,025$, (b) $x=0,05$, $f=1KHz$.

Conclusion

- In the course of this work, we prepared various $BaTiO_3$ derived compositions of the formula $Ba_{1-x}A'_{x/3}A''_{x/3}(Ti_{1-y}B'_y)O_3$ (A' = alcalino-terreux or rare earths ; B' = transition elements). The corresponding ceramics were produced by high-temperature sintering. This study was carried out using homovalent and/or heterovalent substitutions in the octahedral (B) and/or dodecahedral (A) sites of the perovskite $BaTiO_3$.

- The radiocrystallographic study of powder at room temperature enabled us to control the purity of the various solid solutions and to limit their domains of existence. At room temperature, all reflections appearing in the diffractograms are isotypically indexed to BaTiO₃. However, it should be noted that :
 - Reflections from phases exhibiting relaxed ferroelectric behavior are indexed in cubic symmetry.
- Scanning electron microscopy was used to ensure the homogeneity and conformity of the chemical composition of the phases obtained. This study also enabled us to select the optimum sintering conditions.
- The dielectric study carried out over a wide temperature and frequency range revealed the following :
 - Relaxed ferroelectric behavior for solid solutions resulting from mixed substitutions at A and B, Ba_{1-x}A'_{x/3}A''_{x/3}(Ti_{1-y}B'_y)O₃ (A'= Y, Bi, and B'= Zr).
- The dielectric characteristics were determined and then related to the nature and size of the substituted cations. The thermal variation of 1/ε_r' shows a significant deviation from the Curie-Weiss law.
- All the compositions studied are of interest because the corresponding ceramics possess relaxing ferroelectric properties. In addition, these compositions are environmentally friendly and could therefore be used in a wide range of applications.

Replace the lead-based materials currently used in various electronic devices. However, these compounds have relatively low T_m temperature.

- In the future, our planned studies will focus on obtaining high permittivity dielectrics that can be sintered at low temperatures, with near-ambient T_m temperatures and optimum relaxor characteristics. Such materials would be highly attractive in terms of applications. To this end, we have set ourselves the following objectives for future work :
 - Improving sintering conditions.
 - To develop ceramics with coupled substitutions that are conducive to high T_m values.

- [1] Isupov, V.A., 1989. *Ferroelectrics* 90, 113
- [2] Cross, L.E., 1994. *Ferroelectrics* 151, 305.
- [3] Ravez, J., Simon, A., 1997. *Eur. J. Solid State Inorg. Chem.* 34, 1199
- [4] Ravez, J., Simon, A., 2001. *J. Solid State Chem.* 162, 260.
- [5] Jing, Z., et al., *Dielectric properties of Ba (Ti_{1-y}Y_y) O₃ ceramics*. *Journal of applied physics*, 1998. **84**(2): p. 983-986.
- [6] Zhi, J., et al., *Incorporation of yttrium in barium titanate ceramics*. *Journal of the American Ceramic Society*, 1999. **82**(5): p. 1345-1348
- [7] Qi, J., et al., *Yttrium doping behavior in BaTiO₃ ceramics at different sintered temperature*. *Materials chemistry and physics*, 2003. **82**(2): p. 423-427.
- [8] Abrahams, S., S. Kurtz, and P. Jamieson, *Atomic displacement relationship to Curie temperature and spontaneous polarization in displacive ferroelectrics*. *Physical Review*, 1968. **172**(2): p. 551.
- [9] A. Verbaere, Y.P., Z. G. Ye et E. Husson., *Mat. Res. Bull.*, V27, 1227 1992.
- [10] Ravez, J. and A. Simon, *Relaxor-like behavior in highly modified BaTiO₃ ceramics*. *Eur. J. Solid State Inorg. Chem*, 1997. **34**: p. 1199.
- [11] Buscaglia, M.T., et al., *Incorporation of Er³⁺ into BaTiO₃*. *Journal of the American Ceramic Society*, 2002. **85**(6): p. 1569- 1575.
- [12] Tsur, Y., Dunbar, T.D., Randall, C.A., 2001. *J. Electroceramics* 7, 25–34.